Fig. 4. (A) SOD2 mRNA expression in the livers of four mice from each group. (B) Immunoblots of SOD2 and mitochondrial complex I in the mitochondria of four mice from each group after treatment for 6 months. The protein expression levels were normalized against that of mitochondrial heat shock protein 70. $*P < 0.05$ vs control group; $^{\#}P < 0.05$ vs casein/iron group.

In agreement with the antioxidant status, the serum ferritin levels were significantly lower after week 48 of BCAA supplementation (137 ± 109 mg/dl; $P < 0.05$) compared with those before treatment (Table 3). BCAA supplementation significantly increased the serum hepcidin-25 levels at week 48 (20.2 ± 14.5 mg/dl; $P < 0.05$). In addition, we determined the level of albumin synthesis after BCAA supplementation, because the oxidized albumin to total albumin ratio increases with cirrhosis progression and it is related to oxidative stress (32,33). In the present study, there were no differences in the total albumin changes in the non-BCAA or BCAA groups (Table 4). However, the amount of albumin present in the reduced form increased significantly in the BCAA group at week 48 compared with that before the study. By contrast, the level of reduced albumin decreased significantly at week 48 in the non-BCAA group. This suggests that long-term BCAA supplementation reduced iron overload by upregulating antioxidant potential and this improved the albumin status in patients without hypoalbuminaemia and chronic liver failure.

Discussion

Hepatic iron overload and ROS production are both pathophysiological features of HCV-associated chronic liver disease (34) and risk factors for HCC development (35). The reduced hepatic oxidative stress observed after oral BCAA supplementation may be related to changes in the albumin redox state (32, 36). However, previous studies did not determine how BCAA affects iron metabolism and ROS generation.

The mouse model used in the present study shared similarities with the patients who had HCV-associated chronic liver disease in terms of hepatic ROS production and steatosis (14) at 6 months after treatment, followed by hepatocarcinogenesis (15). Furthermore, the hepatic iron concentrations in HCVTgM fed the excess-iron diet were comparable to those of a large number of patients with chronic hepatitis C (30, 37, 38). Thus, HCVTgM fed the excess-iron diet is a suitable model for assessing the effects of long-term supplementation with BCAA on disordered iron metabolism and ROS production in HCV infection.

Table 2. Patient baseline characteristics

	non-BCAA	BCAA	*P*-value
Patients (*N*)	13	12	N.S.
Age (years)	73.5 (65–87)	74.9 (65–83)	N.S.
Sex (male/female)	6/7	6/6	N.S.
White blood cell count ($\times 10^2$/mm^3)	46.2 (30.1–63.4)	45.1 (27.1–84.5)	N.S.
Haemoglobin concentration (g/dl)	13.3 (10.6–16.3)	13.2 (11.4–15.7)	N.S.
Platelet counts ($\times 10^4$/mm^3)	12.2 (4.9–15)	10.5 (3.7–15)	N.S.
Total bilirubin (mg/dl)	0.7 (0.5–1.1)	1.0 (0.3–1.7)	N.S.
Albumin (g/dl)	4.0 (3.5–4.2)	3.9 (3.5–4.2)	N.S.
ALT (IU/L)	33 (23–47)	41 (21–55)	N.S.
AST (IU/L)	43 (32–54)	48 (32–54)	N.S.
ALP (IU/L)	286 (158–435)	302 (145–491)	N.S.
GTP (IU/L)	46 (15–177)	53 (16–137)	N.S.
FBS (mg/dl)	94 (70–130)	107 (72–158)	N.S.
Insulin (μIU/ml)	14 (5.3–39)	14 (6.3–28)	N.S.
Tyrosine (nmol/ml)	104 (76–123)	103 (63–149)	N.S.
BCAA (nmol/ml)	424 (319–606)	401 (269–617)	N.S.
BTR	4.1 (2.6–4.9)	4.0 (2.7–4.4)	N.S.
AFP (ng/dl)	11 (2–61)	18 (2–95)	N.S.
Serum iron (μg/ml)	134 (50–255)	136 (37–256)	N.S.
TSAT (%)	38 (11–70)	44 (12–88)	N.S.
Ferritin (ng/ml)	120 (30–429)	190 (30–346)	N.S.

Results are mean (range). Comparisons between branched-chain amino acids (BCAA) and non-BCAA groups were made using Levene's or Welch's tests. AFP, α-foetoprotein; ALP, alkaline phosphatase; ALT, alanine aminotransferase; AST, aspartate aminotransferase; GGT, gamma glutamyltransferase; BTR, the ratio of BCAA relative to tyrosine; FBS, fasting blood sugar; N.S., Not significant; TSAT, transferrin saturation.

BCAA supplementation improves the nutritional status, prognosis and quality of life for patients with cirrhosis (39, 40). A randomized, controlled trial demonstrated that BCAA supplementation reduced the frequency of HCC in obese male patients with cirrhosis and HCV infection (18). BCAA treatment also reduced the hepatocarcinogenic activity in obese diabetic animals with insulin resistance (9, 10). Insulin resistance promotes hepatocarcinogenesis by activating the mitogen-activated protein kinase (MAPK) pathway and insulin-like growth factor 1 (IGF-1) receptors, which further activates the Raf/MAPK kinase/MAPK cascade (41, 42). BCAA suppress the IGF/IGF-1R axis by downregulating IGF-1, IGF-2 and IGF-1R mRNA expression, thereby leading to the inhibition of mitosis and cell growth (9). BCAA reduce HCC development by inhibiting insulin resistance (43).

In the present study, the FBS levels of HCVTgM fed the excess-iron diet with casein increased after 6 months. BCAA supplementation reduced the iron overload-induced elevation of the FBS. There was no intrahepatic inflation or fibrosis in the HCVTgM fed the excess-iron diet, but those fed the excess-iron diet with casein had significantly lower plasma BCAA levels and a lower BTR compared with those fed excess-iron with BCAA and the control diet. An amino acid imbalance, which is indicated by a lower BTR, has been observed in patients with compensated cirrhosis or chronic hepatitis (44, 45). This suggests that BCAA might potentially reduce hepatic iron accumulation and ROS in patients with HCV-related advanced fibrosis.

Table 3. Changes in oxidative stress and iron metabolism markers during branched-chain amino acids (BCAA) administration*

	Week 0	Week 12	Week 24	Week 48
Hepcidin (ng/ml)				
non-BCAA	11.6 ± 7.9	10.4 ± 9.8	11.8 ± 9.5	10.5 ± 8.8
BCAA	9.5 ± 8.7	9.2 ± 9.5	11.0 ± 9.1	20.2 ± 14.5†
Ferritin (ng/ml)				
non-BCAA	120 ± 121	112 ± 105	100 ± 108	118 ± 120
BCAA	190 ± 135	164 ± 129	163 ± 130	137 ± 109†
Serum iron (μg/ml)				
non-BCAA	134 ± 52	143 ± 60	133 ± 55	142 ± 38
BCAA	136 ± 64	131 ± 63	134 ± 68	117 ± 57
TSAT (%)				
non-BCAA	38 ± 14	42 ± 19	39 ± 15	42 ± 19
BCAA dROM (U.CARR)	45 ± 29	42 ± 24	35 ± 19†	33 ± 16†
non-BCAA	342 ± 64	405 ± 84	431 ± 76†	455 ± 96†
BCAA	360 ± 113	372 ± 80	361 ± 118	359 ± 65
BAP (uM)				
non-BCAA	2369 ± 386	2772 ± 487†	2798 ± 337†	2630 ± 64
BCAA	2139 ± 587	2516 ± 678†	2601 ± 647†	2758 ± 413†
BAP/dROM				
non-BCAA	7.0 ± 1.0	7.1 ± 1.7	6.6 ± 0.7	6.0 ± 1.0†
BCAA	6.1 ± 1.3	6.8 ± 1.5	7.5 ± 1.6†	7.8 ± 1.5†

*Results are mean ± SD.
†*P* < 0.05 vs. before BCAA treatment, Wilcoxon rank-sum test; U.CARR, Cartelli Units (1 U.CARR = 0.8 mg/L of H_2O_2), TSAT, transferrin saturation.

9

Table 4. Changes in the serum albumin characteristics during branched-chain amino acid (BCAA) administration*

	Week 0	Week 12	Week 24	Week 48
Albumin (g/dl)				
non-BCAA (13)	4.0 ± 0.2	4.0 ± 0.2	4.0 ± 0.2	4.0 ± 0.2
BCAA (12)	3.9 ± 0.3	3.8 ± 0.4	3.9 ± 0.3	4.0 ± 0.3
Reduced albumin (%)				
non-BCAA (10)	66 ± 4.5	66 ± 5.3	66 ± 3.9	63 ± 4.9†
BCAA (10)	66 ± 3.9	68 ± 2.8	68 ± 5.2	70 ± 3.2†
Type IV collagen 7s (U/ml)				
non-BCAA (13)	5.8 ± 1.7	6.1 ± 2.5	6.0 ± 2.2	6.1 ± 2.1
BCAA (12)	6.8 ± 2.1	7.1 ± 1.8	7.0 ± 2.1	6.7 ± 2.0
P-III-P (U/ml)				
non-BCAA (13)	0.89 ± 0.19	0.83 ± 0.19	0.91 ± 0.24	0.83 ± 0.15
BCAA (12)	0.88 ± 0.23	0.90 ± 0.16	0.88 ± 0.18	0.86 ± 0.22
Fib4-index				
non-BCAA (13)	5.0 ± 2.7	5.0 ± 2.5	5.4 ± 2.9	5.5 ± 3.7
BCAA (12)	6.8 ± 4.2	7.2 ± 3.7	6.4 ± 4.0	6.3 ± 4.0

*Results are mean ± SD.
†$P < 0.05$ vs. before treatment, Wilcoxon rank-sum test, P-III-P: Type III procollagen peptide.

Our previous study indicated that the antioxidant N-acetylcysteine (NAC) almost completely blocked ROS production and abrogated the hepatic steatosis induced by HCV proteins and iron (30). In the present study, the hepatic triglyceride levels tended to be lower in mice fed the excess-iron diet with BCAA compared with those fed the excess-iron diet with casein, although these differences were not statistically significant ($P = 0.055$). This may have been because BCAA reduce ROS production to a lesser degree than NAC, or because BCAA supplementation did not completely inhibit the ROS-associated unfolded protein response or improve glucose intolerance compared with the control diet. SREBP1 expression is positively regulated by insulin signalling pathways (46). Therefore, further studies are needed to determine whether BCAA reduce hepatic iron accumulation without affecting hepatic steatosis.

CPT1, a transmembrane enzyme in the mitochondrial outer membrane, is negatively regulated at the transcriptional level by malonyl-CoA, which is an intermediate product of fatty acid synthesis (47). Decreased CPT1 expression may be related to the HCV core protein, which is also located in the mitochondrial outer membrane and it generates mitochondrial ROS production indirectly (13). BCAA enhanced protection against mitochondrial injury by restoring the mitochondrial antioxidant potential and mitochondrial complex I activity. Thus, how does BCAA protect from HCV-induced ROS production and mitochondrial injury? The hepatic ROS production increased more in the HCVTgM fed the control diet compared with non-transgenic mice (14), but we did not test whether BCAA supplements reduced ROS production in HCVTgM without the excess-iron diet. However, there were no differences in the liver enzyme, glucose, insulin, BCAA and tyrosine levels of HCVTgM and non-transgenic mice. Furthermore, HCVTgM without the excess-iron diet did not develop severe steatosis and HCC. This indicates that HCVTgM without the excess-iron diet are not a suitable model for long-term treatments with BCAA.

BCAA supplementation increases the reduced form of albumin, which is a predictor of the cirrhosis prognosis (32, 33), while it also improves oxidative stress and iron metabolism in patients with decompensated cirrhosis (36), and in rats exposed to a fibrogenic agent (48). This suggests that the antioxidant effects of BCAA may be related to qualitative changes in serum albumin or the upregulation of albumin synthesis (4, 5, 9, 49). BCAA itself activates the mammalian target of rapamycin, which subsequently upregulates the downstream molecules, eukaryotic initiation factor 4E-binding protein-1 and 70-kDa ribosomal protein S6 kinase, thereby regulating mRNA translation and synthesis (50). In the present clinical study, we confirmed that long-term BCAA supplementation increased the BAP/dROM ratios and serum hepcidin-25 levels, whereas it decreased the serum ferritin levels in patients with HCV-related advanced fibrosis. Moreover, we found that BAP continued to increase from week 12 to week 48, and the level of the reduced albumin form increased at week 48, but without changes in the serum albumin levels, in our BCAA group. The mechanism that allows BCAA to protect against HCV and iron-induced oxidative stress remains uncertain, but BCAA may improve iron metabolism by upregulating the antioxidant potential in patients without decompensated cirrhosis.

In addition, amino acid imbalance is a risk factor for HCC development in patients without hypoalbuminaemia (40), which suggests that BCAA supplementation should be recommended to patients with amino acid imbalances with advanced fibrosis, who may have a decreased antioxidant potential and reduced albumin level. In this study, we could not show any effect by

which BCAA supplementation prevented fibrotic progression (Table 4). However, Fib-4 index in BCAA group at 48 weeks tended to be decreased compared with those at initial point, although these differences were not statistically significant ($P = 0.061$). Long-term BCAAs treatment might inhibit hepatic fibrosis in HCV patients with advanced fibrosis.

Our clinical study had some limitations, including a higher number of older patients who had higher serum albumin and ferritin levels than those in the cohorts reported in other studies, although they used small sample sizes and were not randomized. Further studies should use large cohorts to clarify these effects.

In conclusion, we demonstrated that BCAA administration reduced the hepatic iron contents and ROS levels, which were induced by HCV proteins and iron overloading in mice, probably by protecting the function of mitochondrial complex I. Furthermore, we confirmed that BCAA supplementation improved disordered iron metabolism and the antioxidant status in patients with HCV-related advanced fibrosis. These effects of BCAA may partially account for their inhibitory effects on HCC development in patients with cirrhosis.

Acknowledgements

References

1. Seeff LB. Natural history of chronic hepatitis C. *Hepatology* 2002; **36**: S35–46.
2. Lawitz E, Mangia A, Wyles D, *et al.* Sofosbuvir for previously untreated chronic hepatitis C infection. *N Engl J Med* 2013b; **368**(20): 1878–87.
3. Yamato M, Muto Y, Yoshida T, Kato M, Moriwaki H. Clearance rate of plasma branched-chain amino acids correlates significantly with blood ammonia level in patients with liver cirrhosis. *Int Hepatol Commun* 1995; **3**: 91–6.
4. Nishitani S, Ijichi C, Takehana K, Fujitani S, Sonaka I. Pharmacological activities of branched-chain amino acids: specificity of tissue and signal transduction. *Biochem Biophys Res Commun* 2004; **313**: 387–9.
5. Kuwahata M, Yoshimura T, Sawai Y, *et al.* Localization of polypyrimidine-tract-binding protein is involved in the regulation of albumin synthesis by branched-chain amino acids in HepG2 cells. *J Nutr Biochem* 2008; **19**: 438–47.
6. Nishitani S, Matsumura T, Fujitani S, *et al.* Leucine promotes glucose uptake in skeletal muscles of rats. *Biochem Biophys Res Commun* 2002; **299**: 693–6.
7. She P, Reid TM, Bronson SK, *et al.* Disruption of BCATm in mice leads to increased energy expenditure associated with the activation of a futile protein turnover cycle. *Cell Metab* 2007; **6**: 181–94.
8. Muto Y, Sato S, Watanabe A, *et al.* Overweight and obesity increase the risk for liver cancer in patients with liver cirrhosis and long-term oral supplementation with branched chain amino acid granules inhibits liver carcinogenesis in heavier patients with liver cirrhosis. *Hepatol Res* 2006; **35**: 204–14.
9. Iwasa J, Shimizu M, Shiraki M, *et al.* Dietary supplementation with branched-chain amino acids suppresses diethylnitrosamine-induced liver tumorigenesis in obese and diabetic C57BL/KsJ-db/db mice. *Cancer Sci* 2010; **101**: 460–7.
10. Yoshiji H, Noguchi R, Kaji K, *et al.* Attenuation of insulin-resistance-based hepatocarcinogenesis and angiogenesis by combined treatment with branched-chain amino acids and angiotensin-converting enzyme inhibitor in obese diabetic rats. *J Gastroenterol* 2010; **45**: 443–50.
11. Farinati F, Cardin R, De Maria N, *et al.* Iron storage, lipid peroxidation and glutathione turnover in chronic anti-HCV positive hepatitis. *J Hepatol* 1995; **22**: 449–56.
12. Kato J, Kobune M, Nakamura T, *et al.* Normalization of elevated hepatic 8-hydroxy-2'-deoxyguanosine levels in chronic hepatitis C patients by phlebotomy and low iron diet. *Cancer Res* 2001; **61**: 8697–702.
13. Korenaga M, Wang T, Li Y, *et al.* Hepatitis C virus core protein inhibits mitochondrial electron transport and increases reactive oxygen species (ROS) production. *J Biol Chem* 2005; **280**: 37481–8.
14. Nishina S, Hino K, Korenaga M, *et al.* Hepatitis C virus-induced reactive oxygen species raise hepatic iron level in mice by reducing hepcidin transcription. *Gastroenterology* 2008; **134**: 226–38.
15. Furutani T, Hino K, Okuda M, *et al.* Hepatic iron overload induces hepatocellular carcinoma in transgenic mice expressing the hepatitis C virus polyprotein. *Gastroenterology* 2006; **130**: 2087–98.
16. Beard MR, Abell G, Honda M, *et al.* An infectious molecular clone of a Japanese genotype 1b hepatitis C virus. *Hepatology* 1999; **30**: 316–24.
17. Lerat H, Honda M, Beard MR, *et al.* Steatosis and liver cancer in transgenic mice expressing the structural and nonstructural proteins of hepatitis C virus. *Gastroenterology* 2002; **122**: 352–65.
18. Murao N, Ishigai M, Yasuno H, Shimonaka Y, Aso Y. Simple and sensitive quantification of bioactive peptides in biological matrices using liquid chromatography/selected reaction monitoring mass spectrometry coupled with trichloroacetic acid clean-up. *Rapid Commun Mass Spectrom* 2007; **21**: 4033–8.
19. Bligh EG, Dyer WJ. A rapid method of total lipid extraction and purification. *Can J Biochem Physiol* 1959; **37**: 911–7.
20. Lowry OH, Rosebrough NJ, Farr AL, Randall RJ. Protein measurement with the Folin phenol reagent. *J Biol Chem* 1951; **193**: 265–75.
21. Harrison-Findik DD, Schafer D, Klein E, *et al.* Alcohol metabolism-mediated oxidative stress down-regulates hep-

cidin transcription and leads to increased duodenal iron transporter expression. *J Biol Chem* 2006; **281**: 22974–82.

22. Cesarone MR, Belcaro G, Carratelli M, *et al.* A simple test to monitor oxidative stress. *Int Ang* 1999; **2**: 127–30.

23. Dohi K, Satoh K, Nakamachi T, *et al.* Does edaravone (MCI-186) act as an antioxidant and neuroprotector in experimental traumatic brain injury? *Antioxid Redox Signal* 2007; **8**: 281–7.

24. Jarreta D, Orus J, Barrientos A, *et al.* Mitochondrial function in heart muscle from patients with idiopathic dilated cardiomyopathy. *Cardiovasc Res* 2000; **45**: 860–5.

25. Fujita N, Sugimoto R, Motonishi S, *et al.* Patients with chronic hepatitis C achieving a sustained virological response to peginterferon and ribavirin therapy recover from impaired hepcidin secretion. *J Hepatol* 2008; **49**: 702–10.

26. Pietrangelo A, Dierssen U, Valli L, *et al.* STAT3 is required for IL-6-gp130-dependent activation of hepcidin in vivo. *Gastroenterology* 2007; **132**: 294–300.

27. Wang RH, Li C, Xu X, *et al.* A role of SMAD4 in iron metabolism through the positive regulation of hepcidin expression. *Cell Metab* 2005; **2**: 399–409.

28. Babitt JL, Huang FW, Wrighting DM, *et al.* Bone morphogenetic protein signaling by hemojuvelin regulates hepcidin expression. *Nat Genet* 2006; **38**: 531–9.

29. Miura K, Taura K, Kodama Y, Schnable B, Brenner DA. Hepatitis C virus–induced oxidative stress suppresses hepcidin expression through increase histone deacetylase activity. *Hepatology* 2008; **48**: 1420–9.

30. Nishina S, Korenaga M, Hino K, *et al.* Hepatitis C virus protein and iron overload induce hepatic steatosis through the unfolded protein response in mice. *Liver Int* 2010; **30**: 683–92.

31. Korenaga M, Hidaka I, Nishina S, *et al.* A glycyrrhizin-containing preparation reduces hepatic steatosis induced by hepatitis C virus protein and iron overload in mice. *Liver Int* 2011; **31**: 552–60.

32. Fukushima H, Miwa Y, Shiraki M, *et al.* Oral branched-chain amino acid supplementation improves the oxidized/reduced albumin ratio in patients with liver cirrhosis. *Hepatol Res* 2007; **37**: 765–70.

33. Oettl K, Birner-Gruenberger R, Spindelboeck W, *et al.* Oxidative albumin damage in chronic liver failure: relation to albumin binding capacity, liver dysfunction and survival. *J Hepatol* 2013; **59**: 978–83.

34. Kitase A, Hino K, Furutani T, *et al.* In situ detection of oxidized n-3 polyunsaturated fatty acids in chronic hepatitis C: correlation with hepatic steatosis. *J Gastroenterol* 2005; **40**: 617–24.

35. Kato J, Miyanishi K, Kobune M, *et al.* Long-term phlebotomy with low-iron diet therapy lowers risk of development of hepatocellular carcinoma from chronic hepatitis C. *J Gastroenterol* 2007; **42**: 830–6.

36. Ohno T, Tanaka Y, Sugauchi F, *et al.* Suppressive effect of oral administration of branched-chain amino acid granules on oxidative stress and inflammation in HCV-positive patients with liver cirrhosis. *Hepatol Res* 2008; **38**: 683–8.

37. Hofer H, Osterreicher C, Jessner W, *et al.* Hepatic iron concentration does not predict response to standard and pegylated-IFN/ribavirin therapy in patients with chronic hepatitis C. *J Hepatol* 2004; **40**: 1018–22.

38. Rulyak SJ, Eng SC, Patel K, *et al.* Relationships between hepatic iron content and virologic response in chronic hepatitis C patients treated with interferon and ribavirin. *Am J Gastroenterol* 2005; **100**: 332–7.

39. Kawaguchi T, Izumi N, Charton MR, Sata M. Branched-chain amino acids as pharmacological nutrients in chronic liver disease. *Hepatology* 2011; **54**: 1063–70.

40. Kawaguchi T, Shiraishi K, Ito T, *et al.* Branched-chain amino acids prevent hepatocarcinogenesis and prolong survival of patients with cirrhosis. *Clin Gastroenterol Hepatol* 2014; **12**: 1012-8.e1.

41. Formisano P, Oriente F, Fiory F, *et al.* Insulin-activated protein kinase C beta bypasses Ras and stimulates mitogen-activated protein kinase activity and cell proliferation in muscle cells. *Mol Cell Biol* 2000; **20**: 6323–33.

42. Sandhu MS, Dunger DB, Giovannucci EL. Insulin, insulin-like growth factor-I (IGF-I), IGF binding proteins, their biologic interactions, and colorectal cancer. *J Natl Cancer Inst* 2002; **94**: 972–80.

43. Kawaguchi T, Nagao Y, Matsuoka H, Ide T, Sata M. Branched-chain amino acid-enriched supplementation improves insulin resistance in patients with chronic liver disease. *Int J Mol Med* 2008; **22**: 105–12.

44. Suzuki K, Suzuki K, Koizumi K, *et al.* Measurement of serum branched-chain amino acids to tyrosine ratio level is useful in a prediction of a change of serum albumin level in chronic liver disease. *Hepatol Res* 2008; **38**: 267–72.

45. Michitaka K, Hiraoka A, Kume M, *et al.* Amino acid imbalance in patients with chronic liver diseases. *Hepatol Res* 2010; **40**: 393–8.

46. Kohjima M, Higuchi N, Kato M, *et al.* SREBP-1c, regulated by the insulin and AMPK signaling pathways, plays a role in nonalcoholic fatty liver disease. *Int J Mol Med* 2008; **21**: 507–11.

47. Kerner J, Hoppel C. Fatty acid import into mitochondria. *Biochim Biophys Acta* 2000; **1486**: 1–17.

48. Iwasa M, Kobayashi Y, Mifuji-Moroka R, *et al.* Branched-chain amino acid supplementation reduces oxidative stress and prolongs survival in rats with advanced liver cirrhosis. *PLoS ONE* 2013; **25**(8): e70309.

49. Muto Y, Sato S, Watanabe A, *et al.* Effects of oral branched-chain amino acid granules on event-free survival in patients with liver cirrhosis. *Clin Gastroenterol Hepatol* 2005; **3**: 705–13.

50. Ijichi C, Matsumura T, Tsuji T, Eto Y. Branched-chain amino acids promote albumin synthesis in rat primary hepatocytes through the mTOR signal transduction system. *Biochem Biophys Res Commun* 2003; **303**: 59–64.

Supporting information

Additional Supporting Information may be found in the online version of this article:

Fig. S1. Twenty five patients with HCV-related advanced fibrosis enrolled Human BCAA supplementation study. Advanced fibrosis defined liver specimens (METAVIR fibrosis staging: >F3,4) or Fib-4 index (>3.25).

Fig. S2. HDAC activity of HCV TgM fed the excess-iron diet with BCAA was significantly lower than those of HCVTgM fed the excess-iron diet with casein or the control diet. All samples were nuclear which was extracted from liver tissue.

Sofosbuvir plus ribavirin in Japanese patients with chronic genotype 2 HCV infection: an open-label, phase 3 trial

Masao Omata,[1] Shuhei Nishiguchi,[2] Yoshiyuki Ueno,[3] Hitoshi Mochizuki,[1] Namiki Izumi,[4] Fusao Ikeda,[5] Hidenori Toyoda,[6] Osamu Yokosuka,[7] Kazushige Nirei,[8] Takuya Genda,[9] Takeji Umemura,[10] Tetsuo Takehara,[11] Naoya Sakamoto,[12] Yoichi Nishigaki,[13] Kunio Nakane,[14] Nobuo Toda,[15] Tatsuya Ide,[16] Mikio Yanase,[17] Keisuke Hino,[18] Bing Gao,[19] Kimberly L. Garrison,[19] Hadas Dvory-Sobol,[19] Akinobu Ishizaki,[19] Masa Omote,[19] Diana Brainard,[19] Steven Knox,[19] William T. Symonds,[19] John G. McHutchison,[19] Hiroshi Yatsuhashi[20] and Masashi Mizokami[17] [1]*Yamanashi Prefectural Hospital Organization, Yamanashi, Japan;* [2]*Hyogo College of Medicine, Hyogo, Japan;* [3]*Yamagata University, Yamagata, Japan;* [4]*Musashino Red Cross Hospital, Tokyo, Japan;* [5]*Okayama University, Okayama, Japan;* [6]*Ogaki Municipal Hospital, Gifu, Japan;* [7]*Chiba University, Chiba, Japan;* [8]*Nihon University, Tokyo, Japan;* [9]*Juntendo University, Tokyo, Japan;* [10]*Shinshu University, Nagano, Japan;* [11]*Osaka University, Osaka, Japan;* [12]*Hokkaido University, Hokkaido, Japan;* [13]*Gifu Municipal Hospital, Gifu, Japan;* [14]*Akita City Hospital, Akita, Japan;* [15]*Mitsui Memorial Hospital, Tokyo, Japan;* [16]*Kurume University, Kurume, Japan;* [17]*National Center for Global Health and Medicine, Tokyo, Japan;* [18]*Kawasaki Medical School, Okayama, Japan;* [19]*Gilead Sciences, Inc., Foster City, CA, USA;* and [20]*National Hospital Organization Nagasaki Medical Center, Nagasaki, Japan*

SUMMARY. Genotype 2 hepatitis C virus (HCV) accounts for up to 30% of chronic HCV infections in Japan. The standard of care for patients with genotype 2 HCV – peginterferon and ribavirin for 24 weeks – is poorly tolerated, especially among older patients and those with advanced liver disease. We conducted a phase 3, open-label study to assess the efficacy and safety of an all-oral combination of the NS5B polymerase inhibitor sofosbuvir and ribavirin in patients with chronic genotype 2 HCV infection in Japan. We enrolled 90 treatment-naïve and 63 previously treated patients at 20 sites in Japan. All patients received sofosbuvir 400 mg plus ribavirin (weight-based dosing) for 12 weeks. The primary endpoint was sustained virologic response at 12 weeks after therapy (SVR12). Of the 153 patients enrolled and treated, 60% had HCV genotype 2a, 11% had cirrhosis, and 22% were over the

aged 65 or older. Overall, 148 patients (97%) achieved SVR12. Of the 90 treatment-naïve patients, 88 (98%) achieved SVR12, and of the 63 previously treated patients, 60 (95%) achieved SVR12. The rate of SVR12 was 94% in patients with cirrhosis and in those aged 65 and older. No patients discontinued study treatment due to adverse events. The most common adverse events were nasopharyngitis, anaemia and headache. Twelve weeks of sofosbuvir and ribavirin resulted in high rates of SVR12 in treatment-naïve and previously treated patients with chronic genotype 2 HCV infection. The treatment was safe and well tolerated by patients, including the elderly and those with cirrhosis.

Keywords: Hepatitis C virus, HCV genotype 2, direct-acting antiviral agents, nucleotide polymerase inhibitor.

INTRODUCTION

Approximately two million people in Japan – nearly 2% of the population – are chronically infected with the hepatitis C

virus (HCV) [1]. The population of patients with chronic HCV infection in Japan differs from that of other countries; patients are generally older, have more advanced liver disease and are more likely to have received previous treatment for HCV infection [2,3]. It is estimated that 15–30% of Japanese patients with HCV will develop serious complications, including liver cirrhosis, end-stage liver disease and hepatocellular carcinoma [4]. Although genotype 1 HCV is currently the most prevalent strain of the virus in Japan, genotype 2 HCV, which now accounts for up to 30% of infections, is rising in prevalence [5]. The current standard of care regimen for the treatment of chronic genotype 2 HCV infection in Japan is 24 weeks of pegylated interferon alpha (Peg-IFNα) and ribavirin (RBV) [6]. Although relatively high rates of SVR

have been reported in clinical trials with this regimen (71–86%), the use of Peg-IFNα+RBV in an ageing population with progressive liver disease is limited by safety and tolerability issues. Moreover, a substantial number of patients have absolute or relative contraindications to interferon. As a result, many Japanese patients with chronic genotype 2 HCV infection have no available treatment options and are thus at risk for worsening of liver disease and complications of cirrhosis, including hepatocellular carcinoma.

Sofosbuvir (Gilead Sciences) is an oral nucleotide analogue inhibitor of the HCV-specific NS5B polymerase that has recently been approved in the United States and Europe for the treatment of chronic HCV infection [7]. The labelled use for patients with chronic genotype 2 HCV infection is sofosbuvir and RBV for 12 weeks. In phase 3 studies, 12 weeks of treatment with sofosbuvir plus RBV in patients infected with genotype 2 HCV resulted in rates of SVR12 of 97% in treatment-naïve patients, 93% in patients ineligible to receive interferon and 86–90% in previously treated patients [8–10].

We conducted a phase 3 trial to determine the efficacy and safety of 12 weeks of sofosbuvir and RBV in treatment-naïve and previously treated Japanese patients with chronic genotype 2 HCV infection with and without compensated cirrhosis.

METHODS

Patients

Patients were enrolled between 16 July 2013 and 30 September 2013 at 20 sites in Japan. Eligible patients were aged 20 years or older with a body weight of at least 40 kg. Patients were required to be chronically infected with genotype 2 HCV and with HCV RNA levels $\geq 10^4$ IU/mL at screening. Planned enrolment was for approximately 84 treatment-naïve and 50 previously treated patients. See Supplement for definitions of types of response to prior treatment.

Up to 40% of enrolled subjects in each group (i.e. treatment naive or treatment experienced) could have evidence of compensated cirrhosis at screening (Child-Pugh A). Cirrhosis was defined as liver biopsy showing a Metavir score of 4 or Ishak score ≥ 5 or a FibroScan score of >12.5 kPa. Patients were required to have ALT and AST $\leq 10 \times$ upper limit of the normal range, platelet count $\geq 50\,000$ per μL, haemoglobin ≥ 11 g/dL for women and ≥ 12 g/dL for men and albumin ≥ 3 g/dL. There were no upper limits on age or body mass index. Similarly, no restriction was applied to white blood cell or absolute neutrophil count at screening.

Study design

In this multicenter, open-label trial, all patients received 12 weeks of treatment with 400 mg of sofosbuvir, administered orally once daily, and ribavirin (Copegus®, Chugai

Pharmaceutical Co., Ltd, Tokyo, Japan), administered orally twice daily, with doses determined according to body weight (600 mg daily in patients with a body weight of ≤ 60 kg, 800 mg daily in patients weighing >60 and ≤ 80 kg, and 1000 mg daily in patients with a body weight of >80 kg).

In addition to the main study of efficacy and safety, sparse PK samples were collected from all patients over the course of the study for population PK analyses and all patients were eligible to participate in an optional substudy to determine the steady-state pharmacokinetics (PK) of sofosbuvir (and its predominant circulating metabolite GS-331007). The target enrolment per treatment group was approximately 15 patients. For the PK substudy, intensive serial pharmacokinetic samples were collected (samples obtained over 24 h postdose) at either the week 2 or week 4 treatment visits.

Study assessments

Screening assessments included serum HCV RNA levels and IL28B (rs12979860) genotyping, as well as standard laboratory and clinical tests. Serum HCV RNA was measured with the COBAS® TaqMan® HCV Test, version 2.0 for Use with the High Pure System (Roche Molecular Systems, West Sussex, UK), which has a lower limit of quantification (LLOQ) of 25 IU/mL. HCV genotype and subtype were determined at screening using the Siemens VERSANT HCV Genotype INNO-LiPA 2.0 assay.

On-treatment assessments included standard laboratory testing, serum HCV RNA, vital signs, electrocardiography and symptom-directed physical examinations. All adverse events were recorded and graded according to a standardized scale (see Supplementary Table S7).

NS5B amplification and deep sequencing was performed at DDL Diagnostics Laboratory (Rijswijk, The Netherlands) for all subjects who did not achieve SVR12. Deep sequencing of HCV NS5B was performed at the first virologic failure time point if a plasma/serum sample was available and HCV RNA was >1000 IU/mL, along with the respective baseline samples. Amino acid substitutions in NS5B in the samples collected at virologic failure were compared with the genotype 2 reference and the respective baseline sequence for each patient.

The population pharmacokinetic parameters for sofosbuvir and GS-331007 were computed for all subjects from concentration data from intensive and/or sparse samples using the previously established sofosbuvir and GS-331007 population PK models [11].

Statistical analysis

For treatment-naïve patients without cirrhosis, the SVR12 rate was compared to an adjusted historical SVR rate of 69%, using a two-sided exact one-sample binomial test. The historical control rate was calculated from the weighted average of historical SVR rates for noncirrhotic,

treatment-naïve Japanese patients with genotype 2 HCV infection receiving 24 weeks of Peg-IFNα+RBV (79% with a 10% discount applied due to the expected improvement in safety profile and shorter treatment duration – see Supplementary Table S2 for further details). We calculated that a sample size of 50 patients would provide 80% power to detect an 18% improvement in the SVR12 rate over the adjusted historical rate at a significance level of 0.05. For SVR12 rates for the overall population, for treatment-naïve patients with cirrhosis, and for previously treated patients, statistical hypothesis testing was not performed. For these outcomes, we calculated point estimates of SVR12 rates with two-sided 95% exact confidence interval using the binomial distribution (Clopper–Pearson method).

Study oversight

This trial was approved by the institutional review board or independent ethics committees at all participating sites and was conducted in accordance with local regulations and with recognized international scientific and ethical standards, including the International Conference on Harmonization (ICH) guideline for Good Clinical Practice (GCP)

and the original principles embodied in the Declaration of Helsinki. The study was designed and conducted according to protocol by the sponsor (Gilead Sciences) in collaboration with the principal investigators. The sponsor collected the data, monitored study conduct and performed the statistical analyses. The manuscript was prepared by Gilead Sciences with input from all authors.

RESULTS

Baseline characteristics

Of the 188 patients who were initially screened, 153 (90 treatment-naïve and 63 previously treated patients) were enrolled and began treatment (Table S1 and Figure S1). The demographic and baseline clinical characteristics of the patients are provided in Table 1. Overall, the majority of patients were female (54%), and all were Japanese. The mean age was 57 years (ranging from 25 to 74 years) and 22% were aged 65 or older.

Previously treated patients were slightly older than the treatment-naïve patients, with a higher percentage of males, higher baseline viral load, with a higher prevalence of cirrho-

Table 1 Baseline Demographic Characteristics

Characteristic	Overall ($N = 153$)	Treatment naïve ($n = 90$)	Previously treated ($n = 63$)
Mean age, years (range)	57 (25, 74)	55 (25, 73)	60 (34, 74)
Mean BMI, kg/m^2 (range)	24 (16.5, 34)	24 (17, 34)	24 (16.5, 34)
Male, n (%)	70 (46)	33 (37)	37 (59)
Mean HCV RNA, $\log_{10}$ IU/mL ± SD	6.3 (0.84)	6.2 (0.92)	6.5 (0.66)
HCV RNA ≥5 $\log_{10}$ IU/mL, n (%)	140 (92)	78 (87)	62 (98)
HCV genotype, n (%)			
2a	92 (60)	52 (58%)	40 (63%)
2b	61 (40)	38 (42%)	23 (37%)
Cirrhosis, n (%)			
No	136 (89)	82 (91)	54 (86)
Yes	17 (11)	8 (9)	9 (14)
IL28B genotype, n (%)			
CC	121 (79)	73 (81)	48 (76)
CT	28 (18)	17 (19)	11 (17)
TT	4 (3)	0	4 (6)
Median baseline ALT, U/L (range)	34 (12, 412)	32 (12, 412)	36 (12, 232)
Baseline ALT >1.5 × ULN, n (%)	43 (28)	28 (31)	15 (24)
Interferon eligibility, n (%)*			
Interferon eligible	72 (80)	72 (80)	Not applicable
Interferon ineligible	5 (6)	5 (6)	Not applicable
Interferon unwilling	13 (14)	13 (14)	Not applicable
Response to prior HCV treatment, n (%)			
Nonresponse	15 (24)	Not applicable	15 (24)
Relapse/breakthrough	45 (71)	Not applicable	45 (71)
Interferon intolerant	3 (5)	Not applicable	3 (5)
Median eGFR, mL/min (range)	85 (51, 209)	86 (52, 175)	84 (51, 209)

*Interferon eligibility was determined by the site investigator based on whether or not, in their judgment, the patient had contraindications to interferon therapy.

sis and non-CC IL28B genotype. Overall, 11% of participating subjects had cirrhosis. The proportions of patients infected with genotype 2a and 2b HCV were 60% and 40%, respectively, which is similar to previous reports of HCV subtype distribution in the Japanese population [4]. Most (80%) of the treatment-naïve patients were considered eligible for interferon therapy, with 6% having contraindications to interferon therapy and 14% unwilling to receive this treatment. Most (71%) of the previously treated patients had experienced virologic breakthrough or relapse after previous treatment, with 24% reporting nonresponse to prior therapy.

Efficacy

Overall, 148 of the 153 patients (97%, 95% confidence interval [CI] 93–99%) achieved SVR12 (Table 2). By prior treatment history, 88 of the 90 treatment-naïve patients (98%, 95% CI, 92–100%) and 60 of the 63 previously treated patients (95%, 95% CI, 87–99%) achieved SVR12. Of the 82 treatment-naïve patients without cirrhosis, 80 (97%, 95% CI 91–100%) achieved SVR12, thus meeting the primary efficacy endpoint for this group of superiority to the adjusted historical control rate of 69% ($P < 0.001$). Of note, all eight treatment-naïve patients (100%) with cirrhosis and eight of the nine previously treated patients with cirrhosis (89%) achieved SVR12. Overall, 16 of the 17 patients with cirrhosis (94%, 95% CI 71–100%) achieved SVR12.

Patient responses according to baseline characteristics are shown in Supplementary Table S3. Rates of SVR12 were high in all subgroups of patients. Patients with characteristics historically associated with poor response to interferon-based treatment – non-CC IL28B genotype, high baseline viral load, elderly patients, cirrhosis – had rates of SVR12 similar to those in patients without these characteristics.

Relapse accounted for all cases of virologic failure; there were no patients with virologic breakthrough or nonresponse during treatment. Among all patients treated, 97% had HCV RNA <LLOQ by treatment week 2, and 100% achieved HCV RNA <LLOQ by treatment week 4. Overall, five patients experienced virologic relapse after the end of therapy: two (2%)

treatment-naïve patients and three (5%) treatment-experienced patients. Four patients relapsed by post-treatment week 4, and one patient relapsed between post-treatment weeks 4 and 12. Characteristics of patients who relapsed are provided in Table S4. There were no consistent host or viral characteristics in the five subjects who relapsed; however, the number of virologic failures is too small for any conclusions to be drawn concerning predictors of virologic failure. No patient relapsed after post-treatment week 12. All 148 SVR12 patients (100%) also achieved SVR24.

Viral resistance testing

The NS5B region was deep sequenced in samples collected from the five relapsers at baseline and at the time of relapse. No S282T variant – known to be associated with reduced susceptibility to sofosbuvir – or any other nucleotide inhibitor resistance-associated variants were detected in any patient at relapse. Phenotypic analysis of the NS5B gene showed no change in susceptibility to either sofosbuvir or ribavirin.

Pharmacokinetics

Population pharmacokinetic analysis was performed to estimate the pharmacokinetics of sofosbuvir and its major circulating nucleoside metabolite, GS-331007. The mean (CV%) of steady-state AUC_{0-24} and C_{max} were 973 (31.2) ng*h/mL and 544 (33.6) ng/mL for sofosbuvir ($N = 45$), respectively, and 10 400 (27.2) ng h/mL and 818 (27.9) ng/mL for GS-331007 ($N = 153$), respectively. Within the Japanese study population, there were no clinically relevant differences in the pharmacokinetics of GS-331007 and sofosbuvir, based on age, sex, BMI, cirrhosis status, prior treatment experience or SVR12 outcome.

Safety

Overall, 73% of patients experienced at least one adverse event; however, the majority of patients experiencing

Table 2 Response during and after Treatment

Response	Overall ($N = 153$)	Treatment naïve ($n = 90$)	Previously treated ($n = 63$)
HCV RNA <LLOQ during treatment, n (%)*			
At week 2	148 (97%)	88 (98%)	60 (95%)
At week 4	153 (100%)	90 (100%)	63 (100%)
HCV RNA <LLOQ after end of treatment, n (%)			
SVR4	149 (97%)	89 (99%)	60 (95%)
SVR12	148 (97%)	88 (98%)	60 (95%)
95% confidence interval	92.5–99%	92–>99%	87–99%
On-treatment failure	0	0	0
Relapse, n/n (%)	5 (3%)	2 (2%)	3 (5%)

*LLOQ denotes lower limit of quantification, which is 25 IU/mL. SVR denotes sustained virologic response.

adverse events (84%) had only mild (grade 1) events. The most common treatment-emergent adverse events were nasopharyngitis (upper respiratory viral illness), anaemia, headache, malaise and pruritus (Table 3). No patient in the study discontinued treatment prematurely due to adverse events (or for any other reason). Twenty-two patients (14%) had adverse events that led to modification or interruption of a study drug; 20 patients had ribavirin dose reductions to manage anaemia, and one patient interrupted sofosbuvir and RBV for 1 day because of an event of nasopharyngitis. All but one of the 22 patients with modification or interruption of study drugs achieved SVR12. Two patients experienced treatment-emergent serious adverse events: one treatment-experienced 63-year-old woman had a worsening of anaemia for which she was hospitalized, and one treatment-naïve 36-year-old woman had a severe anaphylactic reaction to a bee sting. No patient experienced a life-threatening (grade 4) adverse event, and only three patients experienced severe (grade 3) events, two of which were deemed to be related to study treatment, the above-mentioned case of anaemia and one case of transient, ribavirin-associated hyperbilirubinaemia in a treatment-experienced 65-year-old man, which resolved during follow-up.

The overall rates of adverse events in younger (<65 years) and older (≥65 years) patients did not differ substantially (72% vs 76%, respectively), although there was a higher incidence of anaemia and pruritus in older

Table 3 Discontinuations, Adverse Events and Laboratory Abnormalities by Age

Parameter	Overall (N = 153)
Discontinuation of any study drug due to adverse event	0
Serious adverse events	2 (1%)
Anaemia	1 (1%)
Anaphylactic reaction	1 (1%)
Any adverse event	112 (73%)
Common adverse events*	
Nasopharyngitis	45 (29%)
Anaemia	18 (12%)
Headache	15 (10%)
Malaise	11 (7%)
Pruritus	9 (6%)
Laboratory abnormalities, n (%)	
Decreased haemoglobin concentration	
<10 g/dL	19 (12%)
<8 g/dL	1 (1%)
Neutropenia (500–<750 per mm^3)	1 (1%)
Hyperglycaemia (>250–500 mg/dL)	3 (2%)
Hyperbilirubinaemia (>2.5–5.0 × ULN)	2 (1%)

ULN, upper limit of normal.
*Adverse events occurring in at least 5% of patients.

patients (Table S5). The incidence and severity of adverse events in patients with and without cirrhosis at baseline were similar (Table S6).

Overall, the mean change in haemoglobin from baseline to week 12 of treatment was −1.2 g/dL. For patients aged 65 and older, the mean change in haemoglobin was −1.7 g/dL, as compared with 1.0 g/dL in patients under the age of 65. Of all 153 patients enrolled and treated, 19 (12%) had at least one postbaseline haemoglobin value of <10.0 g/dL, and one (1%) had a postbaseline haemoglobin value of <8.5 g/dL. Two patients (1%) had grade 3 hyperbilirubinaemia; no grade 4 hyperbilirubinaemia occurred. One patient, who had grade 2 neutropenia at baseline, had transitory grade 3 neutropenia.

DISCUSSION

In this phase 3 trial, twelve weeks of treatment with sofosbuvir and RBV resulted in high rates of sustained virologic response (>95%) in treatment-naïve and previously treated Japanese patients with chronic genotype 2 HCV infection. Patients with host and viral characteristics that have historically been predictive of lower rates of SVR – older age, presence of cirrhosis, high viral load, non-CC IL28B alleles – had rates of SVR12 similar to patients without these characteristics. In patients who had been previously treated for HCV infection, the nature of the prior response was not associated with significant differences in rates of SVR following treatment with sofosbuvir and ribavirin; patients who had nonresponse to prior treatment had similar response rates as patients who had previously experienced relapse or viral breakthrough. No clear or consistent baseline predictors of treatment failure were evident among the five patients who relapsed after treatment.

The current standard-of-care treatment for Japanese patients with chronic genotype 2 HCV infection is 24 weeks of Peg-IFNα+RBV. Although patients who received this regimen in clinical trials achieved SVR12 rates ranging from 72% to 86%, these studies were restricted to patients <65 years of age [12,13]. However, the Japanese population chronically infected with genotype 2 HCV includes many patients with characteristics that make the use of interferon-based therapy problematic – older age, progressive liver disease, prior treatment experience and comorbid conditions such as diabetes and cardiovascular disease [14]. Moreover, many patients cannot receive interferon therapy due to relative or absolute contraindications. The interferon-free combination of sofosbuvir and ribavirin may represent a promising treatment option for these patients.

Given the characteristics of the patient population in Japan with HCV infection – generally older, and more likely to have advanced liver disease – safety and tolerability of therapeutic regimens is an important issue. In the present study, 22% of patients were aged 65 or older and 11% had cirrhosis. Analyses of safety data by age (<65 vs

≥65 years) showed increases in reported adverse events and laboratory abnormalities in older patients, but these differences did not present a barrier to treatment as no premature discontinuation of study treatment occurred in any patient. Analysis of safety data according to the presence or absence of cirrhosis did not indicate clinically important differences in safety or tolerability of the 12-week sofosbuvir plus ribavirin regimen.

Consistent with previous reports, the results of this study confirm the high barrier to resistance afforded by the sofosbuvir plus RBV treatment regimen. Rapid viral suppression was observed with all patients achieving HCV RNA undetectable status by week 4, with no virologic breakthrough observed during treatment in any of the 153 patients. The percentage of patients who relapsed after treatment was low (3%), and none of the subjects who relapsed had S282T or other nucleoside inhibitor resistance-associated variants. No change in susceptibility to sofosbuvir or ribavirin compared with the corresponding baseline or wild-type reference was observed at the relapse time point.

The main limitation of this study was the lack of a control arm to allow direct comparison with interferon-based regimens. Several considerations guided our choice of an uncontrolled study design. Adding an interferon-based control arm would have required exclusion of patients who were ineligible to receive or intolerant of interferon – an important and substantial proportion of patients – as well as previously treated patients, for whom further interferon treatment is not an option. Moreover, given that Peg-IFNα is administered by subcutaneous injection, blinding of treatment arms would not have been possible.

In conclusion, treatment with the all-oral, interferon-free combination of sofosbuvir and RBV resulted in high rates of sustained virologic response in both treatment-naïve and previously treated Japanese patients with chronic genotype 2 HCV infection. The degree of antiviral efficacy coupled with a favourable safety and tolerability profile, including patients with cirrhosis and those aged 65 and older, suggest that this combination may fill an important unmet medical need in Japan.

ACKNOWLEDGMENTS AND DISCLOSURES

REFERENCES

1 Chung H, Ueda T, Kudo M. Changing trends in hepatitis C infection over the past 50 years in Japan. *Intervirology* 2010; 53: 39–43.

2 Tanaka J, Kumgai J, Katayama K *et al.* Sex- and age-specific carriers of hepatitis B and C viruses in Japan estimated by the prevalence in the 3,485,648 first-time blood donors during 1995–2000. *Intervirology* 2004; 47: 32–40.

3 Mizokami M, Tanka Y, Miyakawa Y. Spread times of hepatitis C virus estimated by the molecular clock differ among Japan, the United States and Egypt in reflection of their distinct socioeconomic backgrounds. *Intervirology* 2006; 49: 28–36.

4 Thein HH, Yi Q, Dore GJ, Krahn MD. Estimation of stage-specific fibrosis progression rates in chronic hepatitis C virus infection: a meta-analysis and metaregression. *Hepatology* 2008; 48: 418–431.

5 Toyoda H, Kumada T, Takaguchi K, Shimada N, Tanaka J. Changes in hepatitis C virus genotype distribution in Japan. *Epidemiol Infect* 2014.

6 Kumada H, Okanoue T, Onji M *et al.* Guidelines for the treatment of chronic hepatitis and cirrhosis due to hepatitis C virus infection for the fiscal year 2008 in Japan. *Hepatol Res* 2010; 40: 8–13.

7 Sovaldi (sofosbuvir) Tablets: US Prescribing Information. Foster City, CA: Gilead Sciences, December 2013. Available at: http://www.gilead.com/~/media/Files/pdfs/medicines/liver-disease/sovaldi/sovaldi_pi.pdf.

8 Lawitz E, Mangia S, Wyles D *et al.* Sofosbuvir for previously untreated chronic hepatitis C infection. *N Engl J Med* 2013; 368: 1878–1887.

9 Jacobson IM, Gordon SC, Kowdley KV *et al.* Sofosbuvir for hepatitis C genotype 2 or 3 in patients without treatment options. *N Engl J Med* 2013; 368: 1867–1877.

10 Zeuzem S, Dusheiko GM, Salupere R *et al.* Sofosbuvir and ribavirin in HCV genotypes 2 and 3. *N Engl J Med* 2014; 370: 1993–2001.

11 Kirby B, Gordi T, Symonds WT, Kearney BP, Mathias A. Population pharmacokinetics of sofosbuvir and its major metabolite (GS-331007) in healthy and HCV-infected adult subjects. AASLD Annual Meeting 2013.

12 Kanda T, Imazeki F, Azemoto R *et al.* Response to peginterferon-alfa 2b and ribavirin in Japanese patients with chronic hepatitis C genotype 2. *Dig Dis Sci* 2011; 56: 3335–3342.

13 Inoue Y, Hiramatsu N, Oze T *et al.* Factors affecting efficacy in patients with genotype 2 chronic hepatitis C treated by pegylated interferon alpha-2b and ribavirin: reducing drug doses has no impact on rapid and sustained virological responses. *J Viral Hepat* 2010; 17: 336–344.

14 Asahina Y, Tsuchiya K, Tamaki N *et al.* Effect of aging on risk for hepatocellular carcinoma in chronic hepatitis C virus infection. *Hepatology* 2010; 52: 518–527.

SUPPORTING INFORMATION

Additional Supporting Information may be found in the online version of this article:

Fig. S1. Patient disposition.

Table S1. Reasons for screen failure.

Table S2. Calculation of the adjusted historical control rate.

Table S3. SVR12 by subgroup.

Table S4. Characteristics of patients who relapsed.

Table S5. Common adverse events by age group.

Table S6. Common adverse events by cirrhosis status.

Table S7. Gilead sciences grading scale for severity of adverse events and laboratory abnormalities.

ELSEVIER

GASTROINTESTINAL, HEPATOBILIARY, AND PANCREATIC PATHOLOGY

Hepatitis C Virus Core Protein Suppresses Mitophagy by Interacting with Parkin in the Context of Mitochondrial Depolarization

Yuichi Hara,[*] Izumi Yanatori,[†] Masanori Ikeda,[‡] Emi Kiyokage,[§] Sohji Nishina,[*] Yasuyuki Tomiyama,[*] Kazunori Toida,[§] Fumio Kishi,[†] Nobuyuki Kato,[‡] Michio Imamura,[¶] Kazuaki Chayama,[¶] and Keisuke Hino[*]

From the Departments of Hepatology and Pancreatology,[*] Molecular Genetics,[†] and Anatomy,[§] Kawasaki Medical School, Kurashiki; the Department of Tumor Virology,[‡] Okayama University Graduate School of Medicine, Dentistry and Pharmaceutical Sciences, Okayama; and the Department of Gastroenterology and Metabolism,[¶] Applied Life Sciences, Institute of Biomedical and Health Sciences, Hiroshima University, Hiroshima, Japan

Hepatitis C virus (HCV) causes mitochondrial injury and oxidative stress, and impaired mitochondria are selectively eliminated through autophagy-dependent degradation (mitophagy). We investigated whether HCV affects mitophagy in terms of mitochondrial quality control. The effect of HCV on mitophagy was examined using HCV-Japanese fulminant hepatitis-1—infected cells and the uncoupling reagent carbonyl cyanide m-chlorophenylhydrazone as a mitophagy inducer. In addition, liver cells from transgenic mice expressing the HCV polyprotein and human hepatocyte chimeric mice were examined for mitophagy. Translocation of the E3 ubiquitin ligase Parkin to the mitochondria was impaired without a reduction of pentaerythritol tetranitrate—induced kinase 1 activity in the presence of HCV infection both in vitro and in vivo. Coimmunoprecipitation assays revealed that Parkin associated with the HCV core protein. Furthermore, a Yeast Two-Hybrid assay identified a specific interaction between the HCV core protein and an N-terminal Parkin fragment. Silencing Parkin suppressed HCV core protein expression, suggesting a functional role for the interaction between the HCV core protein and Parkin in HCV propagation. The suppressed Parkin translocation to the mitochondria inhibited mitochondrial ubiquitination, decreased the number of mitochondria sequestered in isolation membranes, and reduced autophagic degradation activity. Through a direct interaction with Parkin, the HCV core protein suppressed mitophagy by inhibiting Parkin translocation to the mitochondria. This inhibition may amplify and sustain HCV-induced mitochondrial injury. (Am J Pathol 2014, 184: 3026—3039; http://dx.doi.org/10.1016/j.ajpath.2014.07.024)

Oxidative stress is present in chronic hepatitis C to a greater degree than in other inflammatory liver diseases.[1,2] The hepatitis C virus (HCV) core protein induces the production of reactive oxygen species (ROS)[3,4] through mitochondrial electron transport inhibition.[5] Because the mitochondria are targets for ROS and ROS generators, HCV-induced ROS have the potential to injure mitochondria. In addition, hepatocellular mitochondrial alterations have been observed in patients with chronic hepatitis C.[6] We previously identified a ROS-associated iron metabolic disorder[7] and demonstrated that transgenic mice expressing the HCV polyprotein develop hepatocarcinogenesis related to mitochondrial injury induced by HCV and iron overload.[8] Therefore, impaired mitochondrial function may play a critical role in

the development of hepatocellular carcinoma (HCC) in patients with chronic HCV infection. Conversely, the affected mitochondria are selectively eliminated through the autophagy-dependent degradation of mitochondria (referred to as mitophagy) in both physiological and pathological settings to maintain the mitochondrial quality.[9,10] On the

basis of these observations, we hypothesized that HCV may suppress mitophagy, which could lead to the sustained presence of affected mitochondria, increased ROS production, and the development of HCC.

Mitochondrial membrane depolarization precedes mitophagy induction,[11] which is selectively controlled by a variety of proteins in mammalian cells, including pentaerythritol tetranitrate—induced kinase 1 (PINK1) and the E3 ubiquitin ligase Parkin.[12-19] PINK1 facilitates Parkin targeting of the depolarized mitochondria.[12-15] Although Parkin ubiquitinates a broad range of mitochondrial outer membrane proteins,[14,17-19] it remains unclear how Parkin enables the damaged mitochondria to be recognized by the autophagosome. Structures containing autophagy-related protein 9A and the uncoordinated family member-51—like kinase 1 complex independently target depolarized mitochondria at the initial stages of Parkin-mediated mitophagy, whereas the autophagosomal microtubule-associated protein light chain 3 (LC3) is critical for efficient incorporation of damaged mitochondria into the autophagosome at a later stage.[20] LC3-I undergoes post-translational modification by phosphatidylethanolamine to become LC3-II, and LC3-II insertion into the autophagosomal membrane is a key step in autophagosome formation. In addition, the autophagic adaptor p62 is recruited to mitochondrial clusters and is essential for mitochondrial clearance,[13] although it remains controversial as to whether p62 is essential for mitochondrial recognition by the autophagosome[13] or rather is important for perinuclear clustering of depolarized mitochondria.[19-21] Our aim was to examine whether HCV suppresses mitophagy. We found that HCV core protein inhibits the translocation of Parkin to affected mitochondria by interacting with Parkin and subsequently suppressing mitophagy. These results imply that mitochondria affected by HCV core protein are unlikely to be eliminated, which may intensify oxidative stress and increase the risk of hepatocarcinogenesis.

Materials and Methods

Cell Culture, HCV Infection Experiments, and Mitochondrial Depolarization

HCV-Japanese fulminant hepatitis-1 (JFH1)—infected Huh7 cells have previously been described in detail.[22] The supernatants were collected from cell culture—generated JFH1-Huh7 cells at 21 days after infection and stored until use at −80°C after filtering through a 0.45-μm filter. For infection experiments with the HCV-JFH1 virus, 1×10^5 Huh7 cells per well were plated onto 6-well plates and cultured for 24 hours. Then, we infected the cells with 50 μL (equivalent to a multiplicity of infection of 0.1) of inoculum. The culture supernatants were collected, and the levels of the HCV core were determined using an enzyme-linked immunosorbent assay (ELISA; Mitsubishi Kagaku Bio-Clinical Laboratories, Tokyo, Japan). Total RNA was isolated from the infected cellular lysates using an RNeasy mini kit (Qiagen, Hilden, Germany) for quantitative

RT-PCR analysis of the intracellular HCV RNA. The HCV infectivity in the culture supernatants was determined by a focus-forming assay at 48 hours after infection. The HCV-infected cells were detected using an anti-HCV core antibody (CP-9 and CP-11, Institute of Immunology, Ltd, Tokyo, Japan). Intracellular HCV infectivity was determined using a focus-forming assay at 48 hours after inoculation of the lysates by repeated freeze-and-thaw cycles (three times).

To depolarize the mitochondria, the cells were treated with 10 μmol/L carbonyl cyanide m-chlorophenylhydrazone (CCCP; Sigma-Aldrich, St. Louis, MO) for 1 to 2 hours or 1 μmol/L valinomycin (Sigma-Aldrich) for 3 hours; CCCP represses ATP synthesis through the loss of the H^+ gradient without affecting mitochondrial electron transport, which is known to induce mitochondrial fragmentation.[13]

Animals

The pAlbSVPA-HCV vector, which contains the full-length polyprotein-coding region under the control of the murine albumin promoter/enhancer, has previously been described in detail.[23,24] Of the four transgenic lineages with evidence of RNA transcription of the full-length HCV-N open reading frame (FL-N), the FL-N/35 lineage proved capable of breeding large numbers.[24] Urokinase-type plasminogen activator—transgenic severe combined immunodeficiency mice were generated, and human hepatocytes were transplanted to generate chimeric mice.[25] The chimeric mice were injected with genotype 1b HCV-positive human serum samples, as described previously.[26] The mouse livers were extracted 12 weeks after the infection, when the serum HCV RNA titers had increased over baseline levels. Male FL-N/35 transgenic mice, age-matched C57BL/6 mice (control), and chimeric mice with and without HCV infection were fed, maintained, and then euthanized by i.p. injection of 10% nembutal sodium, according to the guidelines approved by the Institutional Animal Care and Use Committee. The study protocol for obtaining human serum samples conformed to the ethical guidelines of the 1975 Declaration of Helsinki and was approved by the Institutional Review Committee.

Measurement of HCV RNA and Human Albumin in the Serum of Chimeric Mice

HCV RNA[26] and human albumin[25] were quantified as described previously. Human albumin levels in the serum of chimeric mice were determined using the Human Albumin ELISA Quantification kit (Bethyl Laboratories Inc., Montgomery, TX).

Measurement of Mitochondrial Membrane Potential

The mitochondrial membrane potential ($\Delta\Psi$) was measured using a Cell Meter JC-10 Mitochondrial Membrane Potential Assay kit (AAT Bioquest, Inc., Sunnyvale, CA), according to the manufacturer's instructions. The fluorescent intensities

for both J-aggregates (red) and monometric forms (green) of JC-10 were measured at Ex/Em = 490/525 nm and 540/590 nm with a Varioskan Flush Multimode Reader (Thermo Fisher Scientific, Waltham, MA).

Isolation of Mitochondria

The cells were lysed by mechanical homogenization using a small pestle, and mitochondrial extraction was performed using a Qproteome Mitochondria Isolation kit (Qiagen), according to the manufacturer's instructions. Liver mitochondria were isolated as described previously with some modifications.[27] In brief, the livers were minced on ice and homogenized by five strokes with a Dounce homogenizer and a tight-fitting pestle in isolation buffer [70 mmol/L sucrose, 1 mmol/L KH_2PO_4, 5 mmol/L HEPES, 220 mmol/L mannitol, 5 mmol/L sodium succinate, and 0.1% bovine serum albumin (BSA), pH 7.4]. The homogenate was centrifuged at 800 × g for 5 minutes at 4°C. The supernatant fraction was retained, whereas the pellet was washed with isolation buffer and centrifuged again. The combined supernatant fractions were centrifuged at 1000 × g for 15 minutes at 4°C to obtain a crude mitochondrial pellet.

Measurement of ROS

The cellular ROS level was measured by oxidation of the cell-permeable, oxidation-sensitive fluorogenic precursor, 2′,7′-dihydrodichlorofluorescein diacetate (Molecular Probes Inc., Eugene, OR). Fluorescence was measured using a Varioskan Flush Multimode Reader at 495/535 nm (excitation/emission).

Determination of Glutathione Content

Mitochondrial pellets were measured for total glutathione [reduced glutathione (GSH) + oxidized glutathione (GSSG)] and GSH content using the GSSG/GSH Quantification kit (Dojindo Molecular Technologies, Inc., Kumamoto, Japan). The concentration of GSH was calculated using the following formula:

$$\text{GSH concentration} = \text{Total glutathione concentration}$$
$$- [\text{GSSG concentration}] \times 2 \tag{1}$$

The liver tissue samples (approximately 50 mg) were minced in ice-cold metaphosphoric acid solution, homogenized, and centrifuged at 3000 × g for 10 minutes at 4°C. Lysates from the liver tissue samples and mitochondrial samples (2 mg) were evaluated for the concentration of GSH using the thioester method and a GSH-400 kit (Oxis International Inc., Portland, OR) and for total glutathione content using the glutathione reductase—dinitrothiocyanobenzene recycling assay and the GSH-412 kit (Oxis International Inc.), as described previously.[5]

Immunoblotting

Samples were lysed in radioimmunoprecipitation assay buffer [20 mmol/L Tris-HCl (pH 7.5), 150 mmol/L NaCl,

50 mmol/L NaF, 1 mmol/L Na_3VO_4, 0.1% SDS, and 0.5% Triton X-100], as described previously,[28] supplemented with 1% protease inhibitor mixture (Sigma-Aldrich) and 100 mmol/L phenylmethylsulfonyl fluoride. Cell lysates or mitochondrial pellets were subjected to immunoblot analysis using an iBlot Gel Transfer Device (Invitrogen, Carlsbad, CA). The membranes were incubated with the following primary antibodies: rabbit anti-human LC3 (Novus Biologicals, Littleton, CO), rabbit anti-human p62/SQSTM1 (MBL, Nagoya, Japan), rabbit anti-human Parkin (Cell Signaling Technology, Danvers, MA), mouse anti-human Parkin (Santa Cruz Biotechnology, Inc.), rabbit anti-human p-Parkin (Ser 378; Santa Cruz Biotechnology, Inc.), rabbit anti-human PINK1 (Cell Signaling Technology), mouse anti-human mitochondrial heat shock protein-70 (BioReagents, Golden, CO), mouse anti-human ubiquitin (Santa Cruz Biotechnology, Inc.), goat anti-human voltage-dependent anion-selective channel protein 1 (VDAC1; Santa Cruz Biotechnology, Inc.), monoclonal antisynthetic HCV core peptide (CP11; Institute of Immunology, Ltd), mouse anti-HCV non-structural (NS) 3 protein (Abcam, Cambridge, MA), mouse anti-HCV NS4A (Abcam), mouse anti-HCV NS5A protein (Abcam), and rabbit anti-human β-actin (Cell Signaling Technology).

Electron Microscopy

To address the detail localization of core and Parkin, the cells treated with CCCP for 1 hour were fixed with 4% paraformaldehyde and 1% glutaraldehyde in 0.1 mol/L Millonig's phosphate buffer (pH 7.4) for 30 minutes. The cells were incubated with a mixture of the following primary antibodies in phosphate-buffered saline (PBS) containing 1% BSA and 0.05% sodium azide overnight at 20°C: mouse monoclonal antisynthetic HCV core peptide (Institute of Immunology), rabbit anti-human Parkin (Abcam), and rabbit anti-rat LC3 (Wako Pure Chemical Industries, Ltd, Osaka, Japan). After washing with PBS, the cells were incubated with biotinylated donkey anti-rabbit IgG (Jackson ImmunoResearch Laboratories, Inc., Baltimore Pike, PA) in 1% BSA for 2 hours at 20°C. After washing with PBS, the cells were incubated with Alexa Fluor-488 FluoroNanogold-streptavidin (Jackson ImmunoResearch Laboratories, Inc.), indocarbocyanine-labeled donkey anti-mouse IgG (Jackson ImmunoResearch Laboratories, Inc.), and indocarbocyanine-labeled donkey anti-rabbit IgG (Jackson ImmunoResearch Laboratories, Inc.) in 1% BSA for 2 hours at 20°C. After washing with PBS, the cells were incubated with mouse peroxidase—anti-peroxidase complex (Jackson ImmunoResearch Laboratories, Inc.) in PBS for 3 hours at 20°C. The peroxidase reduction was developed with 0.05% diaminobenzidine tetrahydrochloride in 50 mmol/L Tris buffer containing 0.01% hydrogen peroxide for 20 minutes at room temperature. The diameter of the gold immunoparticles was increased using a silver enhancement kit (HQ silver; Nanoprobes, Inc., Yaphank, NY) for 4 minutes at

room temperature. After treatment with 1% osmium and 2% uranyl acetate, the cells were dehydrated in a graded series of ethanol and embedded in Epon-Araldite (OKEN, Tokyo, Japan). Serial ultrathin sections (each 70 nm thick) were examined using an electron microscope (model JEM1400; JEOL, Tokyo, Japan). These immune—electron microscopic methods were generally performed according to our previous study.[29]

Immunofluorescence Microscopy

The cells were fixed, permeabilized, and immunostained with rabbit anti-human Parkin (Abcam), goat anti-human Parkin (Santa Cruz Biotechnology, Inc.), goat anti-human Tom20 (Santa Cruz Biotechnology, Inc.), rabbit anti-rat LC3 (Wako Pure Chemical Industries, Ltd), or mouse monoclonal anti-synthetic HCV core peptide (Institute of Immunology) antibodies, followed by Cy3-conjugated donkey anti-rabbit IgG (Jackson ImmunoResearch Laboratories, Inc.), fluorescein isothiocyanate—conjugated donkey anti-goat IgG (Jackson ImmunoResearch Laboratories, Inc.), or Alexa Fluor 647—conjugated donkey anti-mouse IgG (Jackson ImmunoResearch Laboratories, Inc.). Cell images were captured using a confocal microscope (model LSM700; Zeiss, Jena, Germany) equipped with 488-, 555-, and 639-nm diodes. The images were acquired in a sequential mode using a 63× Plan Apochromat numerical aperture/1.4 oil objective and the appropriate filter combinations. All images were saved as tagged image file format files. The contrast was adjusted using Photoshop version CS5 (Adobe, San Jose, CA), and the images were imported into Illustrator version CS5 (Adobe). Colocalization was assessed with line scans using ImageJ software version 1.46 (NIH, Bethesda, MD).

Coimmunoprecipitation

Coimmunoprecipitation was performed using a Dynabeads Co-Immunoprecipitation Kit (Invitrogen), according to the manufacturer's instructions. Magnetic beads (Dynabeads M-270 Epoxy) were conjugated to anti-VDAC1 (Santa Cruz Biotechnology, Inc.), anti-Parkin (Cell Signaling Technology), anti-ubiquitin (Santa Cruz Biotechnology, Inc.), or anti-p62 (MBL) antibodies by rotating overnight at 37°C. The antibody-Dynabeads complex was then treated with coupling buffer. Beads coupled to anti-VDAC, anti-Parkin, anti-ubiquitin, or anti-p62 were incubated with cell lysates for 30 minutes at 4°C and then washed with coupling buffer. Collected protein complexes were subjected to immunoblot analysis using anti-VDAC, anti-ubiquitin (Santa Cruz Biotechnology, Inc.), and anti-Parkin (Cell Signaling Technology) antibodies to detect coimmunoprecipitated VDAC1, ubiquitin, and Parkin. Immunoblots using anti-Parkin, anti-HCV core (Institute of Immunology), anti-HCV NS3 (Abcam), anti-HCV NS4A (Abcam), or anti-HCV NS5A (Abcam) antibodies were performed to detect the coimmunoprecipitation of Parkin with core, NS3, NS4A, or NS5A protein.

RNA Interference

The siRNA knockdown oligonucleotides were obtained from Invitrogen. JFH1-Huh7 cells and/or Huh7 cells were grown to 50% to 60% confluency and transfected with 100 pmol siRNA oligonucleotides [5′-GGACGCUGUUCCUCGUUAUGAA-GAA-3′ (forward) and 5′-UUCUUCAUAACGAGGAACA-GCGUCC-3′ (reverse)] for PINK1 or siRNA oligonucleotides [5′-UCCAGCUCAAGGAGGUGGUUGCUAA-3′ (forward) and 5′-UUAGCAACCACCUCCUUGAGCUGGA-3′ (reverse)] for Parkin using Lipofectamine 2000 (Invitrogen). The cells were analyzed 72 hours after transfection.

Yeast Two-Hybrid Assay

A Matchmaker Gal4 two-hybrid system 3 (Clontech Laboratories, Inc., Mountain View, CA) was used according to the manufacturer's instructions. Saccharomyces cerevisiae Y187, containing an N- or C-terminal fragment cDNA of Parkin as a prey cloned into the Gal4-activation domain vector (pACT2), was allowed to mate with S. cerevisiae AH109, which had been transformed with a Gal4 DNA-binding domain vector (pGBKT7) containing the HCV core as bait. In addition, S. cerevisiae Y187, with the HCV core as a prey cloned into the Gal4-activation domain vector (pACT2), was allowed to mate with S. cerevisiae AH109, which had been transformed with a Gal4 DNA-binding domain vector (pGBKT7) containing N- or C-terminal fragment cDNA of Parkin as bait. To construct the prey and the bait, two regions of the Parkin gene that encoded the N-terminal 215—amino acid residues (1 to 215) and the C-terminal 250—amino acid residues (216 to 465) were amplified using PCR with genomic cDNA, and the HCV core gene was amplified with the HCV-O (genotype 1b) genomic cDNA.[30] The PCR primers were as follows with the incorporated BamHI and EcoRI sites underlined: Parkin 1 to 215, 5′-GGATCCGCATGATAGTGTTTGTCAGGTT-3′ (forward) and 5′-GAATTCCTAGTGTGCTCCACATTTAA-AGA-3′ (reverse); Parkin 216 to 465, 5′-GGATCCGCCC-CACCTCTGACAAGGAAAC-3′ (forward) and 5′-GAAT-TCCTACACGTCGAACCAGTGGT-3′ (reverse); and HCV core, 5′-GAATTCGCCATGAGCACAAATCCTAAACCT-C-3′ (forward) and 5′-GGATCCTTAAGCGGAAGCTGG-GATGGTCAAA-3′ (reverse).

Real-Time RT-PCR

Total RNA was extracted from frozen liver tissues and cells using the RNeasy mini kit (Qiagen). Total RNA (2 μg) was reverse transcribed to cDNA using the High-Capacity RNA to cDNA kit (Applied Biosystems, Foster City, CA), according to the manufacturer's instructions. TaqMan Gene Expression Assays for LC3B, glyceraldehyde-3-phosphate dehydrogenase (GAPDH), Parkin, and HCV core were purchased from Applied Biosystems, and mRNA levels were quantified in triplicate using an Applied Biosystems

7500 Real-Time PCR system, according to the supplier's recommendations. The expression value for LC3B, Parkin, and HCV core mRNA was normalized to that of GAPDH.

Statistical Analysis

Quantitative values are expressed as the means ± SD. Data were compared between the two groups using the Student's t-test. $P < 0.05$ was considered significant.

Results

Mitochondrial Oxidative Status *in Vitro* and *in Vivo*

After treatment with CCCP, a widely adopted reagent for inducing mitophagy, the mitochondrial membrane potential ($\Delta\Psi$) was significantly reduced irrespective of HCV infection (Figure 1A). The ratio of reduced/total glutathione content was decreased in the mitochondrial fraction after CCCP treatment in JFH1-Huh7 cells (Figure 1B). Thus, the mitochondrial oxidative status after CCCP treatment was present in HCV-infected cells (JFH1-Huh7). The ratio of reduced/total glutathione content was also decreased in the mitochondrial fraction but not in the whole liver in transgenic mice and HCV-infected chimeric mice compared with the control mice (Figure 1, C and D). These results suggest that there is a baseline oxidation level within the mitochondrial glutathione pool in these transgenic mice and HCV-infected chimeric mice. Furthermore, the mitochondria in these transgenic mice and HCV-infected chimeric mice can undergo mitophagy.

Impaired Recruitment of Parkin to the Mitochondria

Parkin phosphorylation and translocation to the mitochondria after CCCP treatment are indispensable for mitochondrial ubiquitination and subsequent autophagosome formation during the course of mitophagy.[13,15] CCCP exposure induced Parkin accumulation in the mitochondria of Huh7 cells; however, this Parkin recruitment seemed to be inhibited in JFH1-Huh7 cells (Figure 2A). CCCP treatment induces mitochondrial fission, followed by mitophagy.[13] CCCP-treated Huh7 cells displayed fragmented mitochondria colocalized with Parkin, except for a few mitochondrial tubular network cells. Western blot analysis also showed that CCCP-induced recruitment of Parkin to the mitochondria was suppressed without any change in Parkin expression or phosphorylation levels in whole cell lysates of JFH1-Huh7 cells (Figure 2B). Neither CCCP treatment nor HCV infection significantly increased the mRNA levels of Parkin in Huh7 cells, even though there was a tendency of increase in Parkin mRNA after HCV infection (Figure 2C). These results indicate that HCV infection could inhibit Parkin recruitment to CCCP-induced depolarized mitochondria.

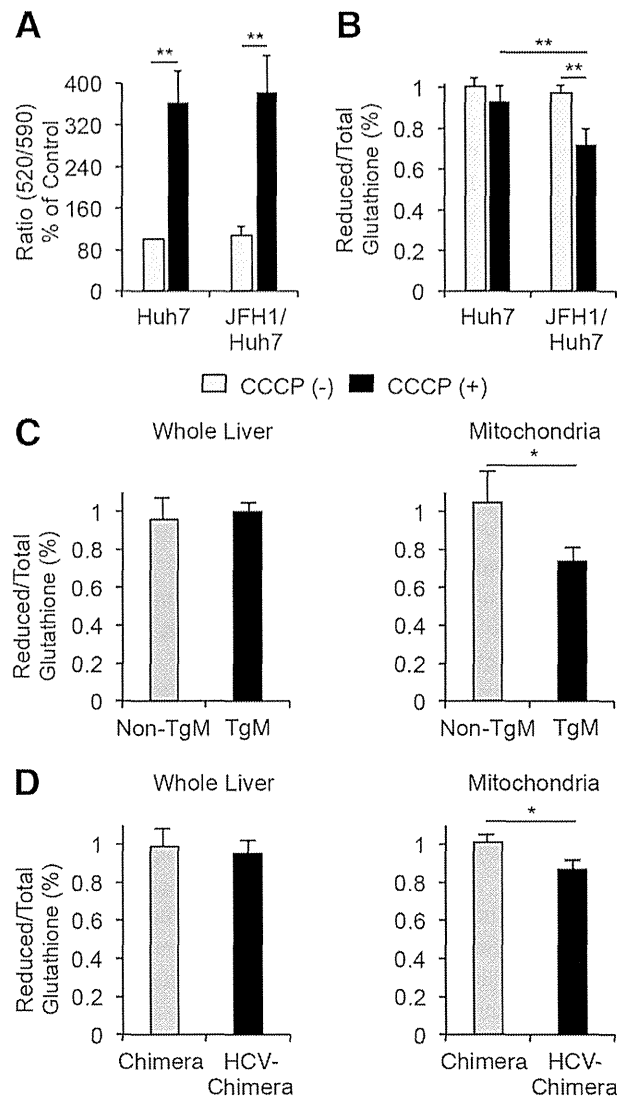The unique and high concentration of CCCP (10 μmol/L) used in the present study may have affected cellular functions

Figure 1 Mitochondrial membrane potential ($\Delta\Psi$) and glutathione content. **A:** Changes in $\Delta\Psi$ levels after a 1-hour carbonyl cyanide *m*-chlorophenylhydrazone (CCCP) treatment for Huh7 and JFH1-Huh7 cells ($n = 5$). The y axis represents the ratio of red (JC-10 aggregate form)/ green (JC-10 monometric form) fluorescence intensity. **B:** Reduced and total glutathione content in mitochondrial fractions ($n = 5$). Reduced glutathione content was normalized to total glutathione content. Reduced and total glutathione content of freshly isolated whole liver homogenates or mitochondrial fractions of transgenic livers ($n = 7$, **C**) or HCV-infected chimeric mice livers ($n = 5$, **D**) compared with the content in the corresponding control liver samples. Reduced glutathione content was normalized to total glutathione content. *$P < 0.05$, **$P < 0.01$.

other than the proton gradient,[31] which suggests that Parkin translocation from the cytoplasm to the mitochondria may not be induced specifically through mitochondrial depolarization. Therefore, we examined mitochondrial accumulation of Parkin using lower CCCP concentrations (0.1, 1, 5, or 10 μmol/L). In coimmunoprecipitation experiments, CCCP exposure induced ubiquitinated Parkin accumulation in the mitochondria in a dose-dependent manner in Huh7 cells, as described previously,[13] but did not induce these changes in JFH1-Huh7 cells (Figure 2D). These results suggest that
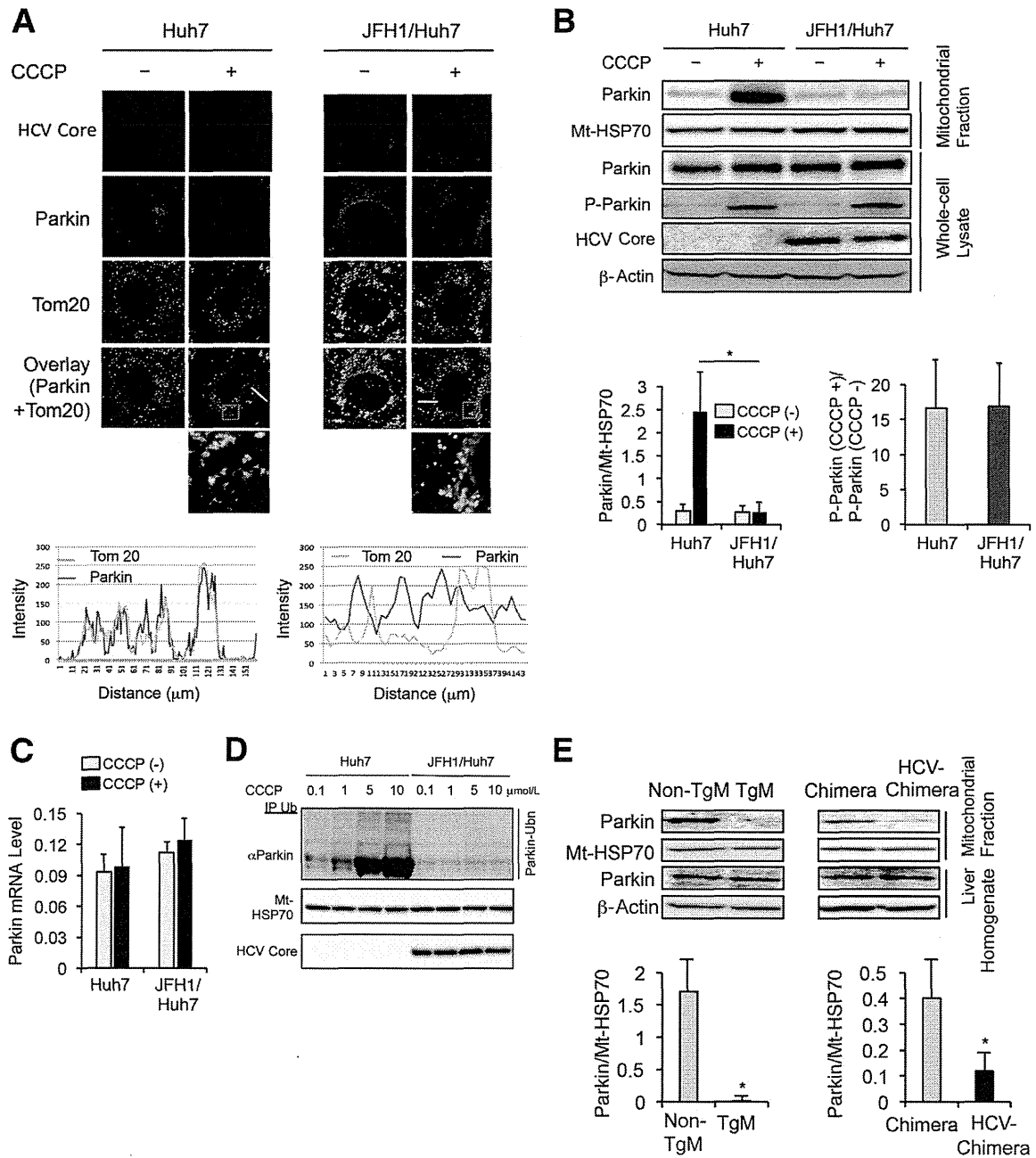
Figure 2 Effect of HCV on the translocation of Parkin to the mitochondria. **A:** Immunofluorescence staining for Parkin (red) and the mitochondrial marker Tom20 (green) in Huh7 and JFH1-Huh7 cells before (−) and after (+) carbonyl cyanide *m*-chlorophenylhydrazone (CCCP) treatment for 1 hour. **Boxed areas** are enlarged below. Endogenous Parkin that colocalizes with the mitochondria (yellow spots). Line scans indicate the colocalization of Parkin with the mitochondria and correlate to the **white lines** in the images. **Boxed areas** are enlarged below. **B:** Immunoblots for Parkin and phosphorylated Parkin (p-Parkin) using the mitochondrial fractions and whole cell lysates before and after CCCP treatment (*n* = 5). Parkin expression level was normalized to mitochondrial heat shock protein 70 (Mt-HSP70). The degree of phosphorylation was expressed as the ratio of phosphorylated Parkin after CCCP treatment to that prior treatment. **C:** Parkin mRNA level in Huh7 cells and JFH1-Huh7 cells before and after CCCP treatment (*n* = 5). The expression level for Parkin was normalized to GAPDH. **D:** Coimmunoprecipitation reveals more ubiquitinated Parkin in CCCP dose-dependent manner in Huh7 cells but not in JFH1-Huh7 cells. **E:** Immunoblots for Parkin using mitochondrial fractions of the livers or liver homogenates from non-TgM and TgM and from chimeric mice with or without HCV infection (*n* = 5 for each type of mouse). $*P < 0.05$.

CCCP specifically induces mitophagy in Huh7 cells and that the HCV infection has an inhibitory effect on mitophagy in JFH1-Huh7 cells.

FL-N/35-transgenic mice and HCV-infected chimeric mice also showed reduced Parkin expression in the mitochondrial fraction of the liver with no change in Parkin

expression levels in whole liver homogenates (Figure 2E). Serum human albumin levels, which serve as useful markers for the extent of replacement with human hepatocytes, were 16.0 ± 7.2 mg/mL in chimeric mice with HCV infection and 11.9 ± 1.7 mg/mL in chimeric mice without HCV infection (Figure 3A). These findings suggest that there was
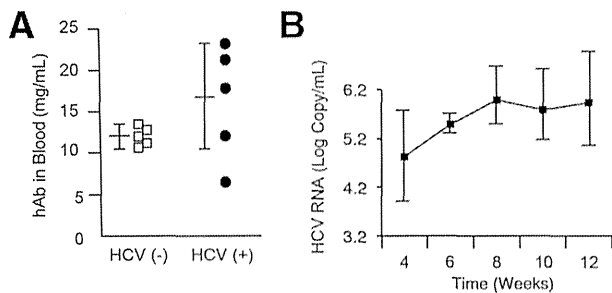
− 411 −

Figure 3 Human albumin and HCV RNA levels in the serum of chimeric mice with or without HCV infection. **A:** Human albumin (hAb) levels in the serum of 3-month-old chimeric mice with or without HCV infection. **B:** Serial change in HCV RNA levels in the serum after HCV infection in chimeric mice ($n = 5$).

a replacement index of >90% according to a graph of the correlation between these two parameters identified in a previous study.[25] Moreover, serum HCV RNA levels increased after infection with HCV (Figure 3B). HCV infection also suppressed the translocation of Parkin to the mitochondria in human hepatocytes.

Interaction between Parkin and the HCV Core Protein

A loss of $\Delta\Psi$ stabilizes the mitochondrial accumulation of PINK1, and PINK1 recruits Parkin from the cytoplasm to depolarized mitochondria via its kinase activity.[11–15] We confirmed that Parkin was phosphorylated to the same degree after CCCP treatment regardless of HCV infection. Therefore, we next examined the mitochondrial accumulation of PINK1. Our results indicate that PINK1 accumulated in the mitochondrial fraction after CCCP treatment, and PINK1 expression levels in whole cell lysates were comparable irrespective of HCV infection (Figure 4A). In

addition, blocking PINK1 protein expression with siRNA (Figure 4B) strikingly suppressed Parkin phosphorylation (Figure 4C) and the mitochondrial Parkin signal after CCCP treatment in Huh7 cells (Figure 4D), indicating that PINK1 recruits Parkin from the cytoplasm to depolarized mitochondria via its kinase activity. Suppressed translocation of Parkin to the mitochondria by HCV infection was also confirmed after treatment with valinomycin, a K^+ ionophore that rapidly dissipates $\Delta\Psi$[32] (Figure 4E).

We next examined the association between HCV protein and Parkin and hypothesized that HCV proteins may suppress Parkin translocation to the mitochondria. Coimmunoprecipitation experiments revealed that Parkin associated with the HCV core protein but not other HCV proteins, such as NS3, NS4A, and NS5A, regardless of CCCP treatment (Figure 5A). These results suggest that the HCV core protein specifically suppressed Parkin translocation to impaired mitochondria by interacting with Parkin.

Finally, we investigated which specific Parkin domain is critical for the interaction with the HCV core protein. The proposed Parkin architecture consists of an N-terminal ubiquitin-like domain, a really interesting new gene (RING) 0 domain (RING0), and a C-terminal in-between RING domain[33] (Figure 5B). Of these domains, the RING0 domain and a complete carboxy-terminal RING configuration are critical for the translocation of Parkin to damaged mitochondria and for consequent mitophagy.[13] By using the HCV core protein as bait and either an N-terminal fragment of Parkin, including RING0 (designated Parkin 1 to 215), or a C-terminal fragment of Parkin, not including RING0 (designated Parkin 216 to 465) as prey, a Yeast Two-Hybrid assay identified a specific interaction between Parkin 1 to 215 and the HCV core protein, which was visualized as a strong blue color (activation of the *MEL1* gene encoding
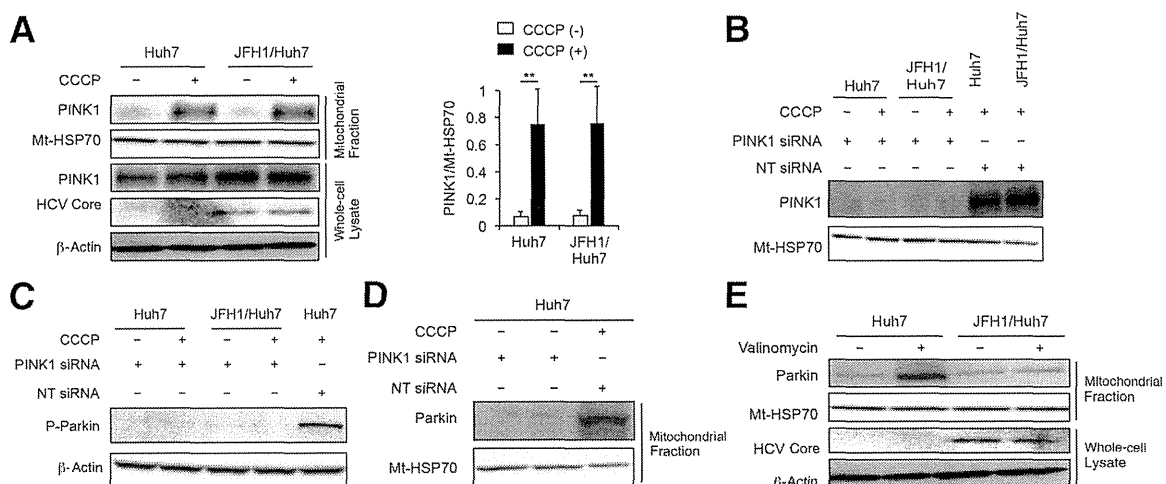

Figure 4 Mitochondrial accumulation of PINK1 after carbonyl cyanide *m*-chlorophenylhydrazone (CCCP) treatment and effect of PINK1 silencing on phosphorylation and mitochondrial translocation of Parkin. **A:** Immunoblots for PINK1 using mitochondrial fractions or whole cell lysates of Huh7 and JFH1-Huh7 cells before and after CCCP treatment ($n = 5$). Immunoblots for PINK1 using mitochondrial fractions (**B**), for phosphorylated Parkin (P-Parkin) using whole cell lysates (**C**), and for Parkin using mitochondrial fractions (**D**) of Huh7 and/or JFH1-Huh7 cells before and after CCCP treatment with or without an siRNA-mediated blockade of PINK1 expression. **E:** Immunoblots for Parkin using the mitochondrial fractions of Huh7 and JFH1-Huh7 cells before and after a 3-hour valinomycin treatment. **$P < 0.01$. Mt-HSP70, mitochondrial heat shock protein 70; NT siRNA, nontargeting siRNA.
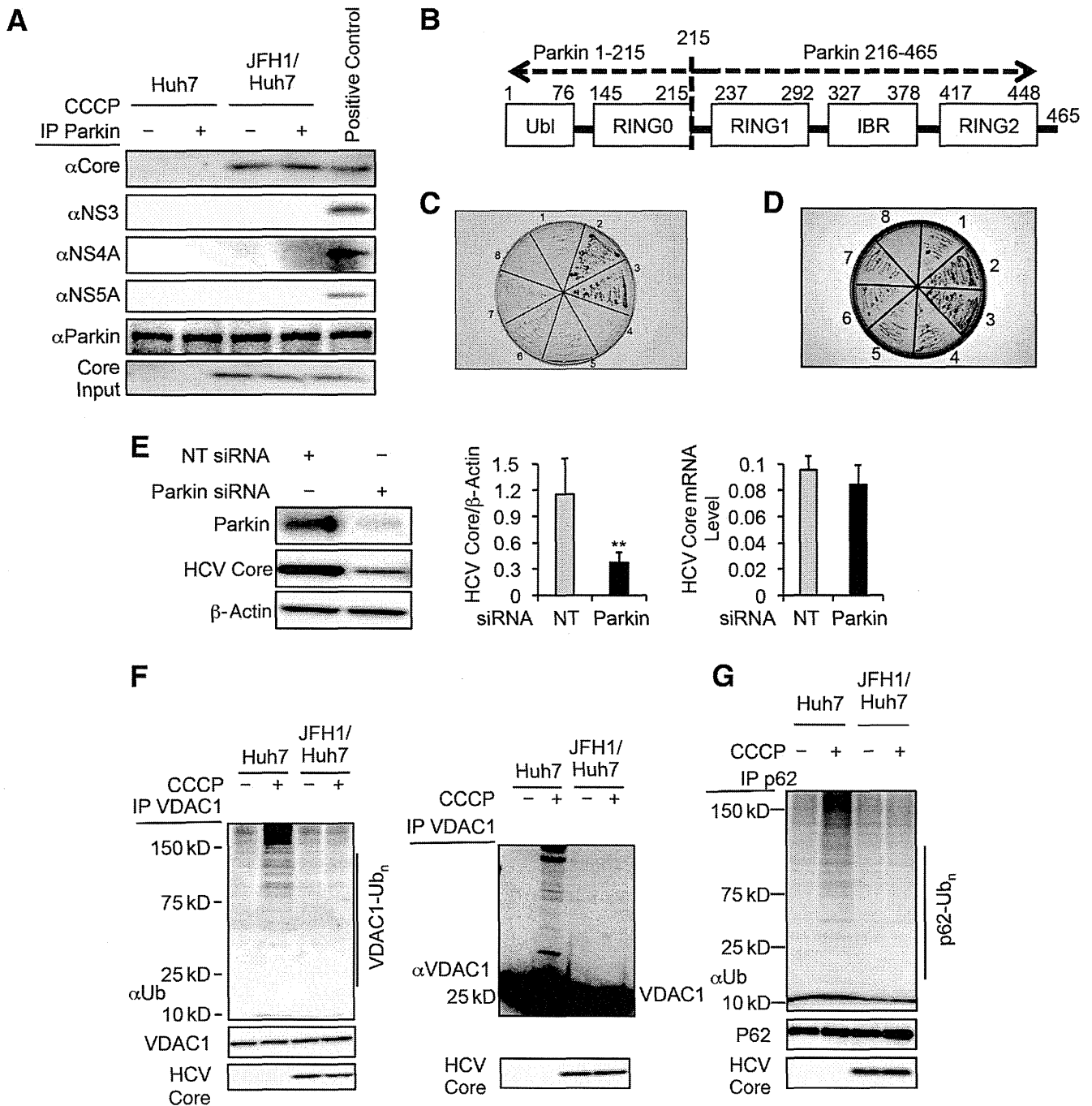
Figure 5 Interaction between Parkin and HCV core protein, effect of Parkin silencing on HCV replication, and reduction of mitochondrial outer membrane ubiquitination. **A:** Coimmunoprecipitation reveals a specific interaction of Parkin with the HCV core protein. **B:** The proposed Parkin architecture and a schematic diagram of Parkin domains. **C** and **D:** A Yeast Two-Hybrid assay identifies a specific interaction between Parkin 1 to 215 and the HCV core protein. The bait and prey for each section (1 to 8) in **C** are as follows: 1, none and none; 2, p53 and large T antigen (positive control); 3, HCV core and Parkin 1 to 215; 4, HCV core and Parkin 216 to 465; 5, HCV core and none; 6, none and Parkin 1 to 215; 7, none and Parkin 216 to 465; 8, no yeast. The bait and prey for each section in **C** were reversed in **D. E:** The HCV core protein and HCV core mRNA levels in JFH1-Huh7 cells with or without an siRNA-mediated blockade of Parkin expression ($n = 5$). **F:** Coimmunoprecipitation reveals more VDAC1 ubiquitination in Huh7 cells after carbonyl cyanide m-chlorophenylhydrazone (CCCP) treatment. Various sizes of VDAC1 immunoprecipitates are also detected by immunoblotting using an anti-VDAC1 antibody in Huh7 cells after CCCP treatment. **G:** Coimmunoprecipitation reveals more p62 ubiquitination in Huh7 cells after CCCP treatment. $**P < 0.01$. IBR, in-between RING; NT, nontargeting siRNA; Parkin, Parkin-targeting siRNA; Ubl, ubiquitin-like.

α-galactosidase) (Figure 5C). In contrast, Parkin 216 to 465 did not interact with the HCV core protein. The same results were found when the core protein was used as prey and different domains of Parkin were used as bait (Figure 5D),

indicating that this interaction between the two proteins was nonpolar. A previous mutational analysis of Parkin revealed that soluble Parkin mutants K211N, T240R, and G430D do not translocate to the mitochondria.[13] Although we have not